Supplementary Materials

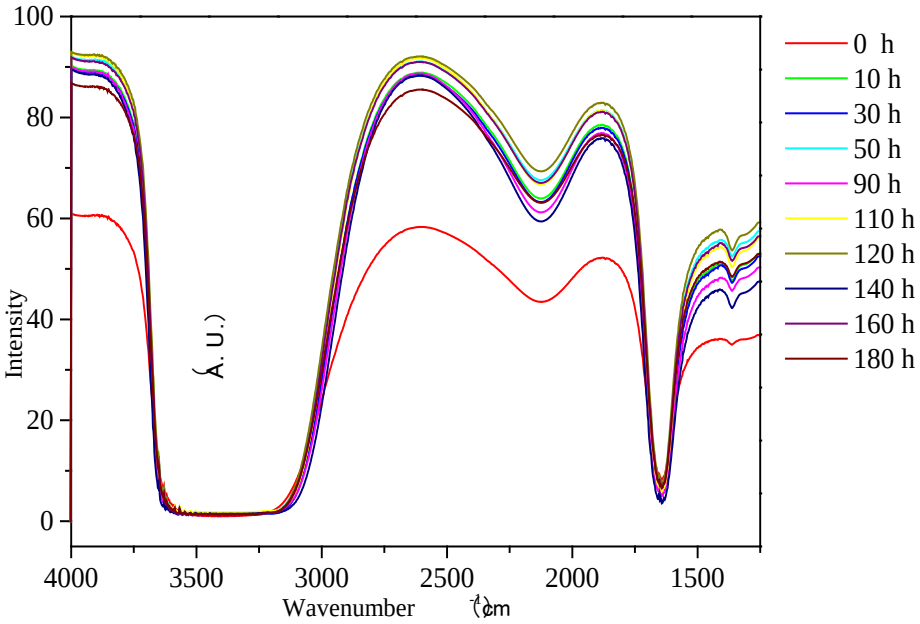

Fig. S1 Time-dependent FTIR spectra during the humification process

Table S1 Assignments of FTIR absorption bands in the humification process

Wavenumber (cm^{-1})	Assignment	Reference
3400	stretching vibration of OH	(Chen et al., 2015; Silva et al., 2020)
2130–2120	stretching vibration of unsaturated groups such as triple bonds and cumulative double bonds	(Abdulla et al., 2010; Li et al., 2014)
1720	C = O stretching of carboxyl and ketonic carbonyls	(Yang et al., 2015; Lee and Hur, 2020)
1660	C = O stretching in conjugation to the aromatic ring	(Amir et al., 2010; Lee and Hur, 2020)
1640	C = O stretching of amide groups in proteins or protein-like compounds, i.e., amide I	(Li et al., 2017)
1606	-COO- stretching of carboxylic acid	(Amir et al., 2010; Li et al., 2014)
1580	C-N stretching and N-H bending vibrations of amide groups in proteins or protein-like compounds, i.e., amide II	(Abdulla et al., 2010; Amir et al., 2010)
1515	Aromatic ring C = C vibrations	(Amir et al., 2010; Li et al., 2014; Yang et al., 2015)
1420	C = N stretching of primary amides, amide III band	(Li et al., 2014; Li et al., 2017; Xu et al., 2018)
1380	OH deformation of phenol-OH and C-O stretching of phenols	(Abdulla et al., 2010)
1350	H deformation of ester C-H bonds (CH_2 and CH_3 groups)	(Chen et al., 2015; Yang et al., 2015)
1190–1180	C-O stretching of phenols	(Amir et al., 2010; Li et al., 2014)

Table S2 DOM fluorescence results for the digestates

Time	Mean component score n[a)] (a.u.)							Relative intensity of fluorescence [b)]				
(h)	C1	C2	C3	C4	C5	R[c)]	Total	C1	C2	C3	C4	C5
0	6.17	10.14	14.78	1.69	2.18	0.76	34.95	0.18	0.29	0.42	0.05	0.06
5	6.42	9.40	14.85	4.97	2.80	0.76	38.44	0.17	0.24	0.39	0.13	0.07
10	6.29	8.42	14.12	5.12	2.91	0.75	36.86	0.17	0.23	0.38	0.14	0.08
20	6.47	8.53	14.23	4.29	3.53	0.73	37.04	0.17	0.23	0.38	0.12	0.10
30	7.09	9.30	14.66	3.45	4.26	0.71	38.77	0.18	0.24	0.38	0.09	0.11
40	6.55	8.76	12.79	3.79	3.96	0.71	35.84	0.18	0.24	0.36	0.11	0.11
50	6.97	9.19	13.64	3.16	4.55	0.69	37.51	0.19	0.25	0.36	0.08	0.12
60	6.60	8.97	11.35	2.61	4.49	0.67	34.03	0.19	0.26	0.33	0.08	0.13
80	6.45	8.65	11.82	2.85	4.60	0.67	34.38	0.19	0.25	0.34	0.08	0.13
100	6.95	8.90	11.50	3.75	4.39	0.68	35.50	0.20	0.25	0.32	0.11	0.12
110	6.94	8.77	12.91	3.85	4.72	0.69	37.18	0.19	0.24	0.35	0.10	0.13
120	6.99	8.83	11.53	4.77	4.84	0.68	36.95	0.19	0.24	0.31	0.13	0.13
125	7.39	8.49	10.47	5.02	4.79	0.66	36.16	0.20	0.23	0.29	0.14	0.13
130	7.08	8.32	9.35	5.66	4.62	0.67	35.03	0.20	0.24	0.27	0.16	0.13
135	7.79	8.95	10.24	4.08	4.94	0.64	36.00	0.22	0.25	0.28	0.11	0.14
140	7.19	8.18	8.04	2.72	4.82	0.61	30.95	0.23	0.26	0.26	0.09	0.16
150	6.21	6.51	4.79	2.79	4.43	0.56	24.73	0.25	0.26	0.19	0.11	0.18
160	6.29	6.99	3.03	3.85	4.74	0.55	24.90	0.25	0.28	0.12	0.15	0.19
170	5.71	5.07	2.99	2.57	4.79	0.5	21.13	0.27	0.24	0.14	0.12	0.23
180	5.64	3.44	1.78	2.16	4.62	0.42	17.65	0.32	0.20	0.10	0.12	0.26

Notes: a) SD-standard deviation. b) Calculated according to Carstea et al. (2014) as a percentage of the total fluorescence. c) Proportion of non-HLAs in the total fluorescence of DOM

References

Abdulla H A, Minor E C, Hatcher P G (2010). Using two-dimensional correlations of 13C NMR and FTIR to investigate changes in the chemical composition of dissolved organic matter along an estuarine transect. Environmental Science & Technology, 44(21): 8044–8049

Amir S, Jouraiphy A, Abdelilah M, Gharous M E, Hafidi M (2010). Structural study of humic acids during composting of activated sludge-green waste: Elemental analysis, FTIR and 13C NMR. Journal of Hazardous Materials, 177(1–3): 524–529

Carstea E M, Baker A, Bieroza M, Reynolds D M, Bridgeman J (2014). Characterisation of dissolved organic matter fluorescence properties by PARAFAC analysis and thermal quenching. Water Research, 61(18): 152–161

Chen W, Habibul N, Liu X Y, Sheng G P, Yu H Q (2015). FTIR and synchronous fluorescence heterospectral two-dimensional correlation analyses on the binding characteristics of copper onto dissolved organic matter. Environmental Science & Technology, 49(4): 2052–2058

Lee Y K, Hur J (2020). Adsorption of microplastic-derived organic matter onto minerals. Water Research, 187: 116426

Li W, Zhang F, Ye Q, Wu D, Wang L, Yu Y, Deng B, Du J (2017). Composition and copper binding properties of aquatic fulvic acids in eutrophic Taihu Lake, China. Chemosphere, 172: 496–504

Li X, Dai X, Takahashi J, Li N, Jin J, Dai L, Dong B (2014). New insight into chemical changes of dissolved organic matter during anaerobic digestion of dewatered sewage sludge using EEM-PARAFAC and two-dimensional FTIR correlation spectroscopy. Bioresource Technology, 159: 412–420

Silva L S D, Constantino I C, Bento L R, Tadini A M, Moreira A B (2020). Humic extracts from hydrochar and Amazonian Anthrosol: Molecular features and metal binding properties using EEM-PARAFAC and 2D FTIR correlation analyses. Chemosphere, 256: 127110

Xu H, Yan M, Li W, Jiang H, Guo L (2018). Dissolved organic matter binding with Pb(II) as characterized by differential spectra and 2D UV-FTIR heterospectral correlation analysis. Water Research, 144: 435–443

Yang L, Han D H, Lee B M, Hur J (2015). Characterizing treated wastewaters of different industries using clustered fluorescence EEM-PARAFAC and FT-IR spectroscopy: implications for downstream impact and source identification. Chemosphere, 127: 222–228